THE ASTROPHYSICAL JOURNAL, 564:1035–1041, 2002 January 10

SECOND HARMONIC EMISSION DURING SOLAR FLARES

ALBERTO M. VÁSQUEZ[1] AND DANIEL O. GÓMEZ[1,2]
Instituto de Astronomía y Física del Espacio, CC 67 Suc 28, (1428) Buenos Aires, Argentina; albert@iafe.uba.ar
AND
CONSTANTINO FERRO FONTÁN[1,2]
Instituto de Física del Plasma, Pabellón I, Ciudad Universitaria, (1428) Buenos Aires, Argentina
Received 1999 April 19; accepted 2001 September 14

ABSTRACT

Type III (type U) radio bursts are signatures of energetic electrons generated during solar flares, traveling along open (closed) magnetic coronal field lines. The burst photons correspond to the second harmonic of the plasma frequency and are generated by the coalescence of two Langmuir waves excited by the beam. In the present paper we derive expressions for the emissivity and absorption in the second harmonic of the plasma frequency without assuming the so-called *head-on* approximation. Only plasma wave isotropy is assumed. The resulting expressions yield important reductions in the emissivity when compared to the head-on results, as well as to lower absorption coefficients. We calculate second harmonic emissivities for several electron beam intensities. The spectrum of Langmuir turbulence used to compute second harmonic emissivity is consistently derived from a model that includes collisional effects and quasilinear relaxation. We speculate that further reductions in the emissivity, down to levels compatible with observations, would be obtained if nonlinear scattering of Langmuir waves with ion-acoustic turbulence and background density inhomogeneities are considered.

Subject headings: Sun: flares — Sun: radio radiation — turbulence

1. INTRODUCTION

Suprathermal electron beams generated during solar flares are known to be responsible for a variety of radiation mechanisms, ranging from hard X-rays (HXRs) to radio frequencies. In particular, these energetic beams are known to generate plasma turbulence by the so-called bump on-tail instability (Tsytovich 1970). Langmuir turbulence, in turn, generates photons at the second harmonic of the local plasma frequency as a result of the coalescence process $L + L' \rightarrow T(2\omega_e)$, where L and L' denote Langmuir waves of different momentum and T denotes a transverse wave at twice the plasma frequency (Kaplan & Tsytovich 1973). Also, the inverse process leads to reabsorption of these photons by the plasma.

The search for mechanisms able to reduce second harmonic emissivity is relevant to the long-standing discrepancy between hard X-rays and microwave intensities generated by a given electron beam. Beam energy fluxes are normally inferred from the HXR intensity generated by the beam, assuming thick target bremsstrahlung. The very good time correlation between HXRs and microwave time series strongly suggests that both emission processes are generated by the same beam. These beams, however, would produce second harmonic emission with typical photon energy fluxes between 1 and 2 orders of magnitude larger than observed levels (Emslie & Smith 1984; Hamilton & Petrosian 1987).

Vásquez & Gómez (1997) developed a model to compute the level of Langmuir turbulence produced by electron beams, consistently considering quasilinear relaxation and collisional effects. They obtain turbulence levels smaller than those derived by Emslie & Smith (1984). Although this result helps to reduce the gap between second harmonic and HXR intensities, it does not remove the discrepancy completely. Therefore, in the present paper we concentrate on the process of second harmonic production, seeking effects able to reduce the emissivity for a given level of Langmuir turbulence.

A semiclassical approach can be used to derive expressions for emissivity and absorption. Previous works on the field (Smith 1970, 1977; Smith & Fung 1971) assume the so-called *head-on* approximation and have been applied to the case of energetic electron beams during solar flares. The head-on approximation is appropriate in cases where the wavenumbers of the Langmuir waves are much larger than the photon characteristic wavenumber, thus implying that the two coalescing Langmuir waves are almost antiparallel. Melrose & Stenhouse (1979) explored the role of the head-on approximation in second harmonic plasma radiation. They find that for power-law Langmuir spectra, sizeable reductions must be expected with respect to the head-on results. Melrose & Stenhouse (1979) study only the emission process, which is sufficient to compute the photon outflow if the coronal conditions in the region of the source can be regarded as optically thin to second harmonic radiation.

In this paper we revisit the expressions for the emissivity and absorption coefficients for second harmonic radiation without assuming head-on. We apply these results to Langmuir spectra generated by flare electron beams, such as those derived by Vásquez & Gómez (1997). In doing so, we assume that the beam-generated Langmuir waves are efficiently isotropized through scattering by thermal ions or ion-acoustic waves. We assume that each individual scattering process produces a small-angle deflection on the Langmuir waves. An alternative mechanism, according to which Langmuir waves experiment backscattering in each interaction, has been analyzed by Cairns (1987). Also under that assumption, the relaxation of the head-on approx-

[1] Also at the Department of Physics, University of Buenos Aires, Argentina.
[2] Member of the Carrera del Investigador, CONICET, Argentina.

imation has been analyzed by Willes, Robinson, & Melrose (1996).

In § 2 we discuss the subject of Langmuir turbulence generated by suprathermal electron beams during solar flares. In § 3 we revisit the general expressions for second harmonic emissivity and absorption. We also rederive the head-on and constant-spectrum as limiting cases, which are approximations commonly found in the literature. In § 4 we apply our results of § 3 to the solar flare spectrum obtained in § 2. Finally, in § 5, we discuss the results thus obtained.

2. BEAM-GENERATED LANGMUIR TURBULENCE

During solar flares, high-energy electron beams are generated. We assume the electron beam to propagate in one dimension, following the magnetic loop field lines. Consistent with this assumption, the beam-generated plasma waves propagate along field lines as well. We take into account the following processes: (1) saturation of the plasma turbulence by the quasilinear relaxation mechanism, and its diffusive effect on the electron distribution function; (2) Coulomb damping on the beam electrons and on the Langmuir waves; (3) nonlinear scattering of Langmuir waves caused by ions and/or ion-acoustic turbulence; and (4) production of second harmonic photons through the $L + L' \rightleftharpoons T(2\omega_e)$ process.

Consistent with these considerations, the set of equations appropriate to describe the steady state situation in terms of the electron distribution function f (normalized so that $n_b = \int dvf$, n_b: beam particle density) and the turbulent spectral energy density W is (Zheleznyakov & Zaitsev 1970)

$$v\frac{\partial f}{\partial x} = \frac{\partial}{\partial v}\left[\frac{\pi\omega_e}{n_e m_e} vW\frac{\partial f}{\partial v} + \nu(v)vf\right], \tag{1}$$

$$v_g\frac{\partial}{\partial x}\frac{W}{\omega_e} = \left(\frac{\pi\omega_e}{n_e}v^2\frac{\partial f}{\partial v} - \nu_L\right)\frac{W}{\omega_e} + \frac{\alpha v^2}{\omega_e}\frac{W}{\omega_e}\frac{\partial}{\partial v}\frac{W}{\omega_e} + \frac{\beta v^4}{\omega_e^2}\left(\frac{W}{\omega_e}\right)^2, \tag{2}$$

where n_e is the particle density, $\omega_e = (4\pi n_e e^2/m_e)^{1/2}$ is the plasma frequency, and e and m_e are the electron charge and mass, respectively. The group velocity of the Langmuir waves is $v_g = \partial\omega(k)/\partial k = 3v_e^2/v$, and $v_e = (k_B T_e/m_e)^{1/2}$ is the electron thermal velocity. The spectral energy density W is defined in such a way that the total energy density for the Langmuir waves is $W_L(\text{ergs cm}^{-3}) = \int W dv$. In equations (1) and (2), the velocity v not only represents the speed of the electrons, but also the phase velocity of plasma waves that are in resonance with the particles. The resonance condition is $v = \omega(k)/k$, where k is the wavenumber of the plasma wave and $\omega(k)$ is given by the dispersion relationship $\omega^2(k) = \omega_e^2 + 3k^2v_e^2$.

The first terms on the right-hand side of equations (1) and (2) describe the beam-wave coupling, while the second terms correspond to collisional damping. The respective collision frequencies, $\nu(v)$ for electrons and ν_L for the Langmuir waves, are (Zheleznyakov & Zaitsev 1970)

$$\nu(v) = \frac{\Lambda\omega_e^4}{8\pi n_e v^3}, \quad \nu_L = \frac{\Lambda\omega_e^4}{16\pi n_e v_e^3}, \tag{3}$$

where $\Lambda \simeq 20$ is the Coulomb logarithm. The typical timescales of this problem are the quasilinear relaxation timescale, $\tau_p^0 \equiv (n_e/n_b)(\pi\omega_e)^{-1}$ (Tsytovich 1970), and the collisional timescale, $\tau_c^0 \equiv 1/\nu(v = v_c)$. In these expressions, v_c is the typical velocity of a suprathermal electron, which corresponds to an energy of around 20 KeV. The coefficient α corresponding to nonlinear scattering by ion-acoustic waves is (Kaplan & Tsytovich 1973)

$$\alpha = \frac{\pi\omega_e^3}{27 n_e m_p v_e^4}. \tag{4}$$

The coefficient for nonlinear scattering by ions is given by the same expression as in equation (4), but divided by a factor $(1 + T_e/T_i)^2$. The coefficient β corresponds to the process $L + L' \rightleftharpoons T(2\omega_e)$ and is given by (Kaplan & Tsytovich 1973)

$$\beta = \frac{\pi\sqrt{3}}{5}\frac{\omega_e^4}{n_e m_e c^5}. \tag{5}$$

Note that the last two processes are represented by quadratic terms in equation (2) Therefore, for sufficiently low beam energy fluxes, which in turn imply low turbulence levels, these two effects could be neglected. Vásquez & Gómez (1997) developed a stationary model in which quasilinear relaxation and collisions are consistently considered. They formulated an iterative procedure to integrate the coupled equations for the electron distribution function and the wave energy density, taking advantage of the fact that quasilinear relaxation occurs on times much shorter than the collisional timescale (i.e., $\tau_p^0 \ll \tau_c^0$). The spectrum of Langmuir waves thus obtained is (see Vásquez & Gómez 1997 for a detailed derivation)

$$W(v, x) = \frac{W_L(x)}{I}\frac{h(v)}{v}, \tag{6}$$

$$h(v) = \tfrac{1}{2}(v^2 - v_1^2)(v_2^2 - v^2), \tag{7}$$

where $v = \omega_e/k$ is the phase velocity of Langmuir waves, v_1 and v_2 are the minimum and maximum phase velocities of the spectrum, respectively, x(cm) denotes the position along the loop field lines (considering $x = 0$ at the point where energetic particles are generated), and

$$I \equiv \int dv\,\frac{h(v)}{v} = \frac{1}{8}\left[v_2^4 - v_1^4 - 4v_1^2 v_2^2 \ln(v1/v2)\right]. \tag{8}$$

In all these expressions, v_1 and v_2 depend (although in a rather smooth fashion) on the energy flux of the injected beam as well as on the temperature of the background.

The spectrum introduced in equation (6) is such that the total energy density in Langmuir waves is $W_L(\text{ergs cm}^{-3}) = \int W(v)dv$. Alternatively, we can also define the spectrum as a function of wavenumbers $W(k)$, under the assumption of an isotropic distribution of waves and so that $W_L(\text{ergs cm}^{-3}) = 4\pi\int W(k)k^2dk$. The relationship between $W(v)$ and $W(k)$ can be obtained in a straightforward fashion, using that $v \approx \omega_e/k$. Figure 1 shows the shape of the spectrum of Langmuir waves $W(k)$ at a given position as a function of wavenumber (in units of $k_t = \sqrt{3}\omega_e/c$).

Detailed computations of the total Langmuir energy density W_L as a function of depth are shown in Vásquez & Gómez (1997). For different values of the electron beam energy flux $\Phi_E(\text{ergs s}^{-1}\text{ cm}^{-2})$, $W_L(x)$ is a smooth function of position, and the dependence of its spatial average on the parameters of the problem is approximately given by

$$\frac{W_L}{n_e k_B T_e} \approx 2.6 \times 10^{-5} n_{10}^{-1/2} T_7^{3/2} \Phi_9^{1.3}, \tag{9}$$

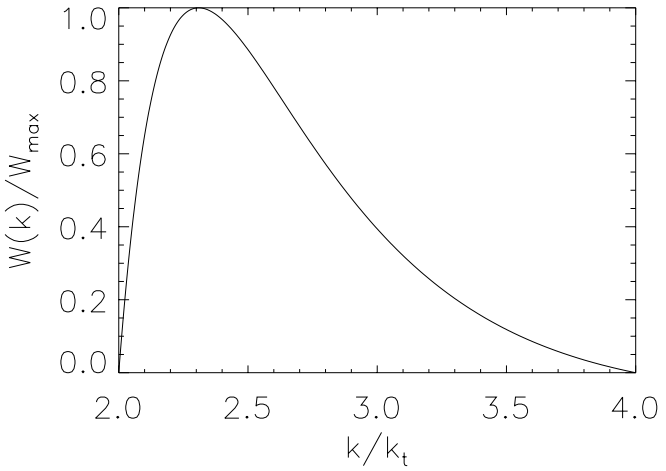

FIG. 1.—Shape of the spectrum of Langmuir waves given by eqs. (6) and (7) as a function of wavenumbers (in units of $k_t = \sqrt{3}\omega_e/c$).

where n_{10} and T_7 are the background electron density and temperature in units of 10^{10} cm^{-3} and 10^7 K, respectively, and Φ_9 is the energy flux of the electron beam in units of 10^9 ergs s^{-1} cm^{-2}. The dependence of the Langmuir turbulence level with the beam intensity like $W_L \propto \Phi_E^{1.3}$ reflects the nonlinearities involved in the resolution of equations (1) and (2).

Once the Langmuir turbulence saturates at the level indicated by equation (9), we assume that the turbulent spectrum becomes isotropic in a virtually instantaneous fashion. There are at least two decay processes that could play this role: (*a*) scattering of Langmuir waves by ions, and (*b*) the electrostatic (ES) decay process $L \leftrightarrow L' + S$ (S: ion-acoustic wave), both of which have been discussed in the literature (see, for example, Tsytovich 1970). Each individual decay is constrained by the conservation of momentum and energy, which poses restrictions on the allowed decays. For the kinematically allowed decays, the rate of occurrence of $L \leftrightarrow L' + S$ can be estimated by computing the rate of generation of S waves, considering both the direct and inverse processes. Using the probability of the decay under analysis (see Tsytovich 1970, Appendix 3), a detailed estimate shows that the decay is fastest for the cases (i.e., equally fast for both cases) of backscattering (L and L' possessing wavevectors almost antiparallel) and small-angle scattering (L and L' possessing wavevectors forming a small angle).

Regardless of whether the dominant isotropization agents are ions or ion-acoustic waves, we assume that the angle between the incoming and outgoing Langmuir waves in each elementary interaction is always small, which allows us to consider isotropization as a diffusion process in wavenumber space. An alternative scenario, according to which Langmuir waves experiment backscattering in each interaction, has been analyzed in detail by Cairns (1987). Under this backscattering assumption, Cairns & Robinson (1995) have also made an analysis of low-frequency wave observations during type III bursts using in situ data obtained by *ISEE 3* at 1 AU. The agreement of their predicted frequencies with the observations lends support to the presence of the ES decay during type III bursts.

In the model of Vásquez & Gómez (1997), the one-dimensional beam-driven Langmuir spectrum is generated on timescales of the order of the quasi-linear relaxation of the beam. On the other hand, estimates for the isotropization times for the two decay processes listed above can be obtained by computing the corresponding rates of occurrence (see Tsytovich 1970, chap. 5). For typical solar flare conditions, these isotropization timescales are about 10–100 times longer than the time for quasi-linear relaxation, which is of order of 10^{-7} s. The assumption of small-angle scattering implies also that the isotropization occurs quasi-elastically, since analogous estimates for the energy transfer time are much larger than the isotropization times.

It is also important to consider the timescale for the coalescence process of Langmuir waves to produce second harmonic radiation. An estimate for this timescale (Tsytovich 1970) results an order of magnitude longer than the isotropization timescale for the most intense beams (three most intense beams on Table 1). Then, for those cases, the angle distribution of Langmuir waves can be considered isotropic. For the less intense case (first line on Table 1) the coalescence and the isotropization timescales can be comparable. In this case, the isotropization process only produces a partial redistribution of orientations, contributing to reduce second harmonic emissivity in comparison to the isotropic case.

To compute an upper bound to the second harmonic production, in what follows we assume the most favorable scenario for the emission process. Therefore, according to this scenario, the beam-driven one-dimensional Langmuir spectrum of equation (6) fully develops and saturates at the level given by equation (9). In a second stage, it becomes isotropic very rapidly, without any significant energy loss, and then the coalescence process produces second harmonic photons.

For the turbulence levels obtained in equation (9), we find that the term proportional to β in equation (2) is indeed very small. This implies that the Langmuir turbulence loses a negligible fraction of its energy to produce second harmonic photons during the development of the turbulence saturation level given by equation (9). This result justifies our approach of computing the Langmuir turbulence level first and calculating the second harmonic emissivity afterward.

On the other hand, in equation (2), the term describing nonlinear scattering (term proportional to α) might be comparable or even larger than the collisional term, at least for sufficiently intense beams. As mentioned above, however, nonlinear scattering has not been considered for the present analysis. Its potential role in the development of the stationary Langmuir spectrum will be addressed in a future paper.

3. SECOND HARMONIC EMISSION

3.1. *Emission and Absorption Coefficients*

Langmuir turbulence generates photons at the second harmonic of the local plasma frequency as a result of the coalescence process $L + L' \rightarrow T(2\omega_e)$. We also consider the inverse process, which involves reabsorption of these photons by the plasma.

To compute the power radiated by the source, we need to solve the corresponding radiative transfer equation. The stationary radiative transfer equation is

$$\frac{dI_\nu}{dr} = J_\nu - \mu_\nu I_\nu , \tag{10}$$

where I_ν is the photon intensity per unit frequency, r is the distance along a ray, $J_\nu = 2\pi J(\boldsymbol{k}_t, \omega)$, and $\mu_\nu = 2\pi\mu(\boldsymbol{k}_t, \omega)$.

The volume emissivity, $J(\boldsymbol{k}_t, \omega)$, is such that $J(\boldsymbol{k}_t, \omega)d\omega d\Omega$ is the power radiated per unit volume in the photon-frequency interval $(\omega, \omega + d\omega)$ in the solid angle $d\Omega$ about the direction of the transverse mode wavevector $\boldsymbol{k}_t$. The inverse process is represented by the absorption coefficient $\mu(\boldsymbol{k}_t, \omega)$.

The aim of this section is to briefly summarize standard formulae for the emissivity and the absorption coefficient, and to compare with the approximate head-on expressions of common use in the literature.

The mathematical expressions for J_v and μ_v can be derived following a semiclassical approach (Smith 1970; Smith & Fung 1971) for a three-plasmon decay process of the type $\sigma_1 + \sigma_2 \rightarrow \sigma$, as sketched in Figure 2.

In our case, $\sigma = t$ is a transverse (electromagnetic) wave and $\sigma_1 = l_1$, $\sigma_2 = l_2$ are Langmuir waves of different momenta. The respective dispersion relationships are

$$\omega_t^2 \approx \omega_e^2 + k_t^2 c^2 , \tag{11}$$

$$\omega_l^2 \approx \omega_e^2 + 3v_e^2 k_l^2 . \tag{12}$$

During this three-wave process, momentum and energy must be conserved. These conditions are conveniently expressed as follows:

$$\boldsymbol{k}_t = \boldsymbol{k}_1 + \boldsymbol{k}_2 , \tag{13}$$

$$\omega_t = \omega_1 + \omega_2 . \tag{14}$$

We define the wave occupation number $N_\sigma(\boldsymbol{k})$ for waves of type σ such that their energy density W^σ is

$$W^\sigma = \int \hbar\omega_\sigma(\boldsymbol{k}) N_\sigma(\boldsymbol{k}) \frac{d\boldsymbol{k}}{(2\pi)^3} = \int W_\sigma(\boldsymbol{k}) d\boldsymbol{k}$$

$$= 4\pi \int dk k^2 W_\sigma(k) , \tag{15}$$

where the last expression holds for the case of isotropic wave turbulence. Also, the total power emitted per unit volume is

$$P^\sigma \equiv \frac{\partial W^\sigma}{\partial t} = \int \hbar\omega_\sigma(\boldsymbol{k}) \frac{\partial N_\sigma}{\partial t}(\boldsymbol{k}) \frac{d\boldsymbol{k}}{(2\pi)^3} \equiv \int d\boldsymbol{k} \frac{P_\sigma(\boldsymbol{k}_t)}{(2\pi)^3} . \tag{16}$$

The process under consideration corresponds to an evolution equation for the occupation number given by

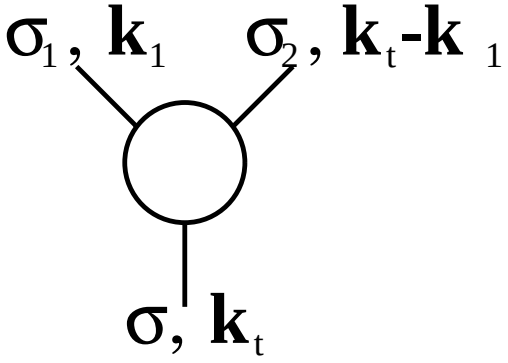

FIG. 2.—Three-plasmon decay interaction. Conservation of momentum is explicitly displayed.

(Tsytovich 1970)

$$\frac{\partial N_\sigma}{\partial t}(\boldsymbol{k}_t) + v_g \frac{\partial N_\sigma}{\partial r}(\boldsymbol{k}_t) = \int w_\sigma^{\sigma_1 \sigma_2} [N_{\sigma_1}(\boldsymbol{k}_1) N_{\sigma_2}(\boldsymbol{k}_2)$$

$$- N_{\sigma_1}(\boldsymbol{k}_1) N_\sigma(\boldsymbol{k}_t) - N_{\sigma_2}(\boldsymbol{k}_2) N_\sigma(\boldsymbol{k}_t)] \frac{d\boldsymbol{k}_1 \, d\boldsymbol{k}_2}{(2\pi)^6} , \tag{17}$$

where $w_\sigma^{\sigma_1 \sigma_2}$ is the probability for the coalescence of the waves σ_1 and σ_2 to generate the wave σ, and it is given by

$$w_\sigma^{\sigma_1 \sigma_2}(\boldsymbol{k}_t, \boldsymbol{k}_1, \boldsymbol{k}_2) = \frac{\hbar e^2 (2\pi)^6}{32\pi m_e^2} \frac{(k_1^2 - k_2^2)^2}{k_t^2 \omega_e} \frac{|\boldsymbol{k}_1 \times \boldsymbol{k}_2|^2}{k_1^2 k_2^2}$$

$$\times \delta(\boldsymbol{k}_t - \boldsymbol{k}_1 - \boldsymbol{k}_2) \delta(\omega_t - \omega_{\sigma_1} - \omega_{\sigma_2}) . \tag{18}$$

The three terms in the right-hand side of equation (17) represent the direct process (emission, positive term) and the inverse process (absorption, negative terms). The expression of $J(\boldsymbol{k}_t, \omega)$ as a function of the occupation number $N_\sigma(\boldsymbol{k})$ can be derived considering that the power emitted per unit volume must also be given by

$$P^\sigma = \int d\Omega d\omega J(\boldsymbol{k}_t, \omega) . \tag{19}$$

From equations (16) and (19), and considering that the emissivity corresponds to the first term of the right-hand side of equation (17), we obtain

$$J(\boldsymbol{k}_t, \omega) = \frac{k_t^2}{d\omega/dk_t} \int \frac{d\boldsymbol{k}_1 \, d\boldsymbol{k}_2}{(2\pi)^9} \hbar\omega_\sigma w_\sigma^{\sigma_1 \sigma_2} N_{\sigma_1}(\boldsymbol{k}_1) N_{\sigma_2}(\boldsymbol{k}_2) . \tag{20}$$

The expression for $\mu(\boldsymbol{k}_t, \omega)$ can be derived in a similar fashion, associating the absorption process to the second and third terms of the right-hand side of equation (17), to obtain

$$\mu(\boldsymbol{k}_t, \omega) = \frac{1}{d\omega/dk_t} \int \frac{d\boldsymbol{k}_1 \, d\boldsymbol{k}_2}{(2\pi)^6} w_\sigma^{\sigma_1 \sigma_2} [N_{\sigma_1}(\boldsymbol{k}_1) + N_{\sigma_2}(\boldsymbol{k}_2)] . \tag{21}$$

Using equation (15) we can cast equations (20) and (21) in terms of $W_\sigma(\boldsymbol{k})$:

$$J(\boldsymbol{k}_t, \omega) = \frac{k_t^2}{d\omega/dk_t} \frac{1}{\hbar(2\pi)^3}$$

$$\times \int d\boldsymbol{k}_1 \, d\boldsymbol{k}_2 \frac{\omega_\sigma(\boldsymbol{k}_t)}{\omega_{\sigma_1}(\boldsymbol{k}_1)\omega_{\sigma_2}(\boldsymbol{k}_2)} w_\sigma^{\sigma_1 \sigma_2} W_{\sigma_1}(\boldsymbol{k}_1) W_{\sigma_2}(\boldsymbol{k}_2) , \tag{22}$$

$$\mu(\boldsymbol{k}_t, \omega) = \frac{1}{d\omega/dk_t} \frac{1}{\hbar(2\pi)^3}$$

$$\times \int d\boldsymbol{k}_1 \, d\boldsymbol{k}_2 \, w_\sigma^{\sigma_1 \sigma_2} \left[\frac{W_{\sigma_1}(\boldsymbol{k}_1)}{\omega_{\sigma_1}(\boldsymbol{k}_1)} + \frac{W_{\sigma_2}(\boldsymbol{k}_2)}{\omega_{\sigma_2}(\boldsymbol{k}_2)} \right] . \tag{23}$$

3.2. *Isotropic Langmuir Spectra*

Replacing the probability given by equation (18) into equations (22) and (23), the integrals in $\boldsymbol{k}_2$ can easily be performed using the conservation of momentum. To obtain the total emissivity and absorption rates, we integrate equa-

tions (22) and (23) in ω. To this end, we use the conservation of energy for this three-wave process, and we take into account the corresponding dispersion relationships given by equations (11) and (12). The following results are obtained, where we explicitly assume the Langmuir wave distribution to be isotropic:

$$J_t \equiv \int d\omega J(\boldsymbol{k}_t, \omega) = \frac{\pi}{4 n_e m_e c \sqrt{3}} \times \int_{-1}^{+1} \int_0^{\infty} 2\pi d\eta k_1^2 \, dk_1 \, F(k_1, \eta) W_l(k_1) W_l(|\boldsymbol{k}_t - \boldsymbol{k}_1|) , \quad (24)$$

$$\mu_t \equiv \int d\omega \mu(\boldsymbol{k}_t, \omega) = \frac{\pi c}{24\sqrt{3} n_e m_e \omega_e^2} \times \int_{-1}^{+1} \int_0^{\infty} 2\pi d\eta k_1^2 \, dk_1 \, F(k_1, \eta)[W_l(k_1) + W_l(|\boldsymbol{k}_t - \boldsymbol{k}_1|)] . \quad (25)$$

We have defined

$$F(k_1, \eta) \equiv \frac{[\boldsymbol{k}_1 \times (\boldsymbol{k}_t - \boldsymbol{k}_1)]^2}{\boldsymbol{k}_1^2 (\boldsymbol{k}_t - \boldsymbol{k}_1)^2} [\boldsymbol{k}_1^2 - (\boldsymbol{k}_t - \boldsymbol{k}_1)^2]^2 = \left(1 - \frac{k_1^2 + k_t^2 \eta^2 - 2 k_t k_1 \eta}{k_1^2 + k_t^2 - 2 k_t k_1 \eta}\right)(2 k_t k_1 \eta - k_t^2)^2 , \quad (26)$$

where η is the cosine of the (variable) angle between $\boldsymbol{k}_t$ (fixed) and $\boldsymbol{k}_1$ (variable). Note, for instance, that for $\eta = 1$ (i.e., $\boldsymbol{k}_1 \| \boldsymbol{k}_t \| \boldsymbol{k}_2$) there is no emission, which can also be seen directly form the expression for the decay probability given in equation (18), which clearly drops to zero in this case.

The integrals involved in equations (24) and (25) depend on the shape of the turbulent spectrum. Before computing J_t and μ_t for any particular Langmuir spectrum, we turn our attention to the head-on approximation to test its validity in typical flaring conditions.

3.3. *The Head-on Approximation*

The head-on approximation is valid for Langmuir wavenumbers much larger than the transverse wavenumber $k_t \approx \sqrt{3}\omega_e/c$. This approximate expression for k_t is a direct consequence of the conservation of energy (equation [14]) and the dispersion relationship for the transverse plasmons (equation [11]). Using $k_t \ll k_1, k_2$, the kernel $F^{\rm ho}(k_1, \eta)$ in the head-on approximation becomes (see also Melrose & Stenhouse 1979)

$$F^{\rm ho}(k_1, \eta) \approx (\boldsymbol{k}_t \times \boldsymbol{k}_1)^2 \frac{4(\boldsymbol{k}_1 \cdot \boldsymbol{k}_t)^2}{\boldsymbol{k}_1^4} = 4 k_t^4 \eta^2 (1 - \eta^2) . \quad (27)$$

Other standard approximation in the $k_t \ll k_{1,2}$ case is $W_l(|\boldsymbol{k}_t - \boldsymbol{k}_1|) \approx W_l(k_1)$. In this limit, the double integrals involved in equations (24) and (25) become decoupled (regardless of the shape of the turbulent spectrum), and the angular integration can be performed analytically, yielding $\int d\eta F^{\rm ho} = (16/15) k_t^4$. Thus, the expressions for emissivity and absorption in the head-on approximation become

$$J_t^{\rm ho} = \frac{8\pi^2}{15\sqrt{3} n_e m_e c} k_t^4 \int_0^{\infty} dk_1 \, k_1^2 \, W_l^2(k_1) , \quad (28)$$

$$\mu_t^{\rm ho} = \frac{8\pi^2 c}{45\sqrt{3} n_e m_e \omega_e^2} k_t^4 \int_0^{\infty} dk_1 \, k_1^2 \, W_l(k_1) . \quad (29)$$

To test the validity of the head-on approximation, in the next section we compare, for the particular turbulent spectrum derived in § 2, the results obtained from the more general equations (24) and (25) with those derived from equations (28) and (29).

3.4. *Constant Langmuir Spectrum*

If we further assume the Langmuir spectrum to be broad and constant (a common approximation in the existing literature), we obtain

$$J_t^K \approx \frac{1}{10} \frac{\omega_e W_{\rm L}^2}{n_e m_e c^2} \left(\frac{k_t}{k_m}\right)^3 , \quad (30)$$

$$\mu_t^K \approx \frac{\sqrt{3}\pi}{15} 2 \frac{\omega_e^2 W_{\rm L}}{n_e m_e c^3} , \quad (31)$$

where $W_{\rm L}$ (ergs cm^{-3}) is the total energy density in Langmuir turbulence and k_m is the maximum wavenumber of the spectrum. Equation (30) for emissivity has been used in previous studies (Smith & Spicer 1979; Emslie & Smith 1984). Note, however, that our expression for the absorption coefficient (eq. [31]) is a factor of ~ 7 smaller the one reported by Smith & Spicer (1979).

4. RESULTS FOR BEAM-GENERATED LANGMUIR TURBULENCE IN SOLAR FLARES

In § 2, we computed the energy density level of Langmuir waves generated by a suprathermal electron beam during solar flares. In § 3, we obtained general expressions for second harmonic emissivity. To obtain the intensity of second harmonic emission during solar flares, we replace the turbulent spectrum given by equations (6), (7), and (8) in our expressions for the emissivity and absorption coefficients (given by eqs. [24] and [25]). Note that the spectrum $W(v, x)$ in equation (6) is expressed as a function of the phase velocity v, while in equations (24) and (25) we use $W(k, x)$. Replacing into the expressions for the emissivity and absorption coefficients, we obtain

$$J_t = \frac{1}{32} \frac{I_J}{I^2} \left(\frac{\omega_e W_{\rm L}^2}{n_e m_e c^2}\right) , \quad (32)$$

$$\mu_t = \frac{\sqrt{3}\pi}{16} \frac{I_\mu}{I} \left(\frac{\omega_e^2 W_{\rm L}}{n_e m_e c^3}\right) , \quad (33)$$

where we have defined the integrals

$$I_J \equiv \frac{1}{k_t} \int_{-1}^{+1} d\eta \int_0^{\infty} dk_1 \frac{F(k_1, \eta)}{k_1 k_2^3} h(\omega_e/k_1) h(\omega_e/k_2) , \quad (34)$$

$$I_\mu \equiv \frac{1}{k_t^4} \int_{-1}^{+1} d\eta \int_0^{\infty} dk_1 \, F(k_1, \eta) k_1^2 \left[\frac{h(\omega_e/k_1)}{k_1^3} + \frac{h(\omega_e/k_2)}{k_2^3}\right] , \quad (35)$$

and $k_2 = |\boldsymbol{k}_t - \boldsymbol{k}_1| = (k_t^2 + k_1^2 - 2 k_1 k_t \eta)^{1/2}$.

Equations (32) and (33) can also be used for the head-on limiting case provided that the integrals I_J and I_μ are replaced by their head-on versions:

$$I_J^{\rm ho} = \frac{16}{15} k_t^3 \int_0^{\infty} dk_1 \frac{h(\omega_e/k_1)^2}{k_1^4} , \quad (36)$$

$$I_\mu^{\rm ho} = \frac{32}{15} \int_0^{\infty} dk_1 \frac{h(\omega_e/k_1)}{k_1} . \quad (37)$$

TABLE 1

MAXIMUM WAVENUMBERS

Φ_9[a] ($\times 10^9$ ergs s^{-1} cm^{-2})	k_{max}/k_t
1	3.5
5	3.9
10	4.1
50	4.9

[a] Beam energy flux.

Since the head-on limit has become a standard approximation in the literature, we are interested in testing its validity for typical flare situations. To this end, we now compute the ratios:

$$\rho_J \equiv J/J^{ho} = I_J/I_J^{ho} , \quad (38)$$

$$\rho_\mu \equiv \mu/\mu^{ho} = I_\mu/I_\mu^{ho} . \quad (39)$$

For a typical electron beam of ~ 20 keV, the minimum wavenumber of the spectrum is $k_{min}/k_t \sim 2.07$. We computed the integrals for the following beam injection energy fluxes Φ_E: 1, 5, 10, and 50×10^9 ergs s^{-1} cm^{-2}. In each case, the generated Langmuir spectrum has different maximum wavenumbers k_{max}, depending both on the injection energy flux and the background electron temperature. In all cases we consider $T \sim 10^7$ K as a typical temperature for a flaring loop. As a result, for the various cases we studied (see Vásquez & Gómez 1997), the maximum wavenumbers obtained are shown in Table 1.

It is clear that in all these cases, the wavenumber ranges for the Langmuir spectra do not satisfy the requirements for the head-on approximation (as $k_{min}/k_t \sim 2.07$). In Figure 3 we show the ratio of emission (absorption) between the exact and the head-on cases J/J_t^{ho} (μ/μ^{ho}) as a function of k_{max}/k_t. It can be seen that in a typical case of $k_{max}/k_t \sim 4$ (see Table 1), the emissivity is reduced by a a factor of ~ 2.

Comparing both panels of Figure 3 we see that the head-on approximation breaks down more noticeably for emission than for absorption. This result arises from the nonlinear dependence of emission with turbulent spectra, while for absorption the dependence is linear (see eqs. [28] and [29]). In Figure 4, we show the ratio of emission between the exact and the head-on cases J/J_t^{ho} as a function of minimum and maximum wavenumbers.

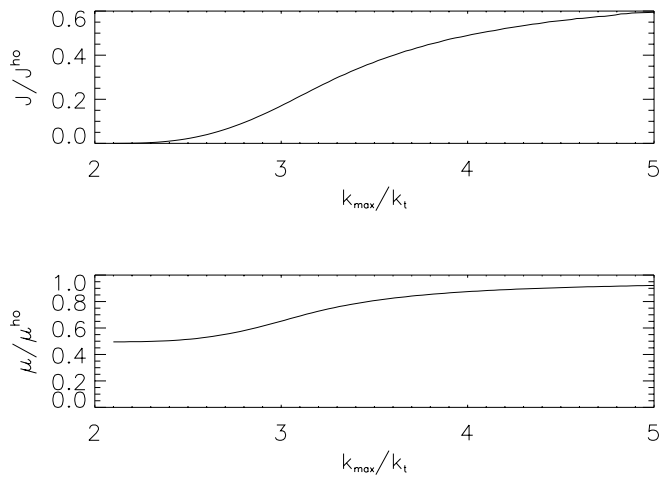

FIG. 3.—For $k_{min}/k_t \sim 2.07$, corresponding to a beam cutoff energy of 20 keV, we show the ratio of emission (absorption) between the exact and the head-on cases J/J_t^{ho} (μ/μ^{ho}) as a function of maximum wavenumbers. The calculations were made for the turbulent spectrum given by eq. (6).

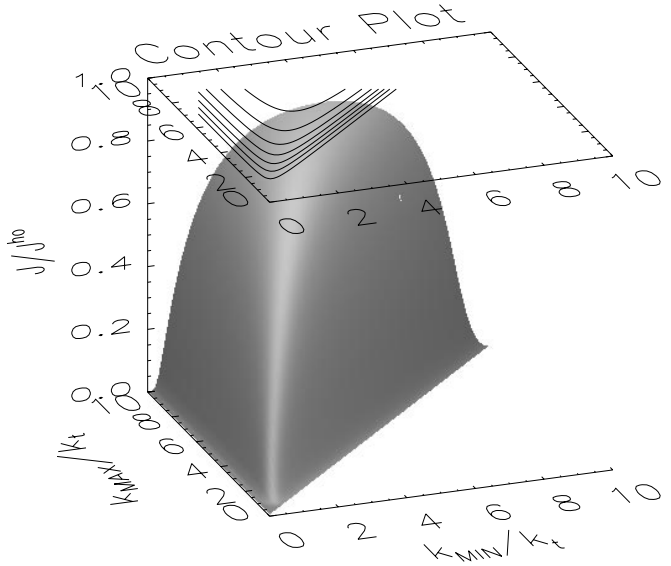

FIG. 4.—Ratio of emission between the exact and the head-on cases J/J_t^{ho} as a function of minimum and maximum wavenumbers. On the top of this figure, seven contour plots for reduction factors of 0.1, 0.2, …, 0.7 are displayed. The calculations were made for the turbulent spectrum given by eq. (6).

On the top of this figure, seven contour plots for reduction factors of 0.1, 0.2, …, 0.7 are displayed. It can be seen that as both k_{min} and k_{max} grow, the ratio of emission between the exact and head-on cases tends asymptotically toward unity because, in this limit, the head-on approximation becomes valid.

5. DISCUSSION AND CONCLUSIONS

Type III and type U radio bursts are the signatures of energetic electrons generated during flares, traveling along open or closed magnetic fieldlines, respectively. The coalescence of two Langmuir waves excited by the beam produces a photon at the second harmonic of the plasma frequency. In the case of type U bursts, these electron beams eventually hit the transition region where they are collisionally stopped, producing HXR signatures through nonthermal bremsstrahlung. Thus, typical beam intensities are derived from HXR observations.

One of the unsolved problems in solar physics is the fact that electron beams with typical intensities inferred from HXR data yield second harmonic emissivities much larger than observed levels. In the present paper we derive expressions for the emissivity and absorption in the second harmonic of the plasma frequency without assuming the head-on approximation. We calculate second harmonic emissivities for several electron beam intensities. To compute the corresponding levels of Langmuir turbulence, we use the model developed by Vásquez & Gómez (1997). In all the cases studied, we show that the head-on assumption is not adequate, and that our more general expressions lead to sizeable reductions in the second harmonic emissivity.

We assume that the beam-generated Langmuir waves are efficiently isotropized through scattering by thermal ions or

ion-acoustic waves (ES decay). We assume that each elementary interaction produces a small-angle deflection on the Langmuir waves. The resulting expressions yield, in certain spectral regions, to important reductions in the emissivity when compared to the head-on results, as well as lower absorption coefficients. An alternative mechanism, according to which Langmuir waves experiment backscattering in each interaction, has been analyzed by Cairns (1987). Under this backscattering assumption, the relaxation of the head-on approximation has been analyzed by Willes et al. (1996). Their study has led to an increase in second harmonic emissivity. As pointed out in § 2, there is observational evidence supporting the presence of the ES decay during type III bursts. Assuming backscattering, Cairns & Robinson (1995) obtain a reasonable agreement between their theoretically predicted IA frequencies and in situ measurements of plasma waves (during type III bursts) in the 100–300 Hz range, taken by *ISEE 3* at 1 AU. Small-angle decay processes could in principle explain observations of relatively smaller frequencies, also present during type III bursts. An example of this are the low-frequency bursts detected by *Ulysses* in the 25–60 Hz range (see Thejappa & MacDowall 1998). A more general model, including all possible angles between incoming and outgoing Langmuir waves, is certainly necessary to obtain more definite results. In any case, other effects should be considered as well, such as nonlinearities and background inhomogeneities, as discussed below.

For the present study, the level of Langmuir turbulence has been computed under the so-called quasilinear approximation. Therefore, we neglected nonlinear effects such as scattering of Langmuir waves caused by ions or ion-acoustic waves. For typical beam intensities, this effect might become comparable or even larger than the collisional damping of Langmuir waves. We postpone a detailed study of the relevance of nonlinear scattering in the development of a stationary Langmuir spectrum for a future paper. We speculate, however, that the inclusion of this effect might lead to further reductions in second harmonic emissivity. The effect of the term proportional to α in the propagation of Langmuir waves described by equation (2) will be to skew the Langmuir spectrum displayed in Figure 1, progressively shifting its "center of mass" to larger velocities (i.e., smaller wavenumbers). Since second harmonic emissivity is proportional to $W(|\boldsymbol{k}|)W(|\boldsymbol{k}_t - \boldsymbol{k}|)$ (as shown in eq. [24]), a higher degree of skewness in $W(k)$ contributes to a reduction in the emissivity.

Another factor that could seriously affect the emissivity is related to the isotropization mechanism of the beam-driven one-dimensional Langmuir spectrum. We proposed, as reasonable isotropization agents, the scattering of Langmuir waves through ions or ion-acoustic waves. In § 2 we presented a conservative scenario by assuming that the isotropization timescales are slower than the quasilinear relaxation timescale. However, sufficiently large pressures or sufficiently intense beams can in principle reduce the isotropization timescales to levels comparable to the quasilinear relaxation timescales. Under these circumstances, the isotropization mechanisms also contribute to take Langmuir waves off resonance, thus reducing the energy density in Langmuir waves to levels smaller than indicated by equation (9).

We also assumed that the background density is a smooth function of the distance along the flaring loop. This is also a conservative assumption, since it is likely that the density displays a "clumpy" behavior with a complex distribution of density gradients. Whenever the beam travels through an inhomogeneous region, the local plasma frequency changes accordingly and the Langmuir waves suddenly become out of resonance with the beam. Robinson, Cairns, & Gurnett (1992) (see also Robinson 1992; Robinson, Cairnes, & Willes 1994) have developed a stochastic growth theory of type III source regions that is able to incorporate the observed fragmented character of these phenomena. In particular, see Robinson, Cairns, & Gurnett (1993) for their predictions on the clumpy character of the excited Langmuir wave and a detailed comparison with observations. This effect also reduces the saturation level of the Langmuir spectrum with respect to the one given by equation (9).

Therefore, either faster isotropization or an inhomogeneous density distribution contribute to reduce the turbulence level, which in turn reduces second harmonic emissivity. In summary, although an adequate computation of the level of Langmuir turbulence produced by a beam and the relaxation of the head-on assumption lead to important reductions in second harmonic emissivity, it seems apparent that more research is necessary to explain the long-standing discrepancy between HXR and second harmonic emissivities.

This work was supported by CONICET grant PIP 4519/99 to IAFE and by grant TX 065/98 from the University of Buenos Aires to the Department of Physics. We thank to the Smithsonian Astrophysical Observatory and Fundación Antorchas for partial support. We also express our thanks to the referee for his/her constructive comments, which helped to clarify some key issues of this manuscript.

REFERENCES

Cairns, I. H. 1987, J. Plasma Phys., 38, 179
Cairns, I. H., & Robinson, P. A. 1995, ApJ, 453, 959
Emslie, A. G., & Smith, D. F. 1984, ApJ, 279, 882
Hamilton, R. J., & Petrosian, V. 1987, ApJ, 321, 721
Kaplan, S. A., & Tsytovich, V. N. 1973, Plasma Astrophysics (Oxford: Pergamon)
Melrose, D. B., & Stenhouse, J. E. 1979, A&A, 73, 151
Robinson, P. A. 1992, Sol. Phys., 139, 147
Robinson, P. A., Cairns, I. H., & Gurnett, D. A. 1992, ApJ, 387, L101
———. 1993, ApJ, 407, 790
Robinson, P. A., Cairns, I. H., & Willes, A. J. 1994, ApJ, 422, 870
Smith, D. F. 1970, Adv. Astron. Astrophys., 7, 147
———. 1977, ApJ, 216, L53
Smith, D. F., & Fung, P. C. W. 1971, J. Plasma Phys., 5, 1
Smith, D. F., & Spicer, D. S. 1979, Sol. Phys., 62, 359
Thejappa, G., & MacDowall, R. J. 1998, ApJ, 498, 465
Tsytovich, V. N. 1970, Nonlinear Effects in Plasma (New York: Plenum)
Vásquez, A. M., & Gómez, D. O. 1997, ApJ, 484, 463
Willes, A. J., Robinson, P. A., & Melrose, D. B. 1996, Phys. Plasmas, 3, 149
Zheleznyakov, V. V., & Zaitsev, V. V. 1970, Soviet Astron., 14, 47